DRAFT VERSION FEBRUARY 2, 2008
Preprint typeset using LaTeX style emulateapj v. 04/03/99

arXiv:astro-ph/0210408v1 17 Oct 2002

THE DISCOVERY OF A SPATIALLY-RESOLVED SUPERNOVA REMNANT IN M31 WITH *Chandra*

ALBERT K.H. KONG, MICHAEL R. GARCIA, FRANCIS A. PRIMINI AND STEPHEN S. MURRAY
Harvard-Smithsonian Center for Astrophysics, 60 Garden Street, Cambridge, MA 02138; akong@cfa.harvard.edu

Draft version February 2, 2008

ABSTRACT

Chandra observations of M31 allow the first spatially resolved X-ray image of a supernova remnant (SNR) in an external spiral galaxy. CXOM31 J004327.7+411829 is a slightly elongated ring-shaped object with a diameter of $\sim 11''$ (42 pc). In addition, the X-ray image hints that the chemical composition of the SNR is spatial dependent. The X-ray spectrum of the SNR can be well fitted with a Raymond-Smith model or a non-equilibrium ionization model. Depending on the spectral model, the 0.3–7 keV luminosity is between 3.2×10^{36} erg s^{-1} and 4.5×10^{37} erg s^{-1}. The age of the SNR is estimated to be 3210–22300 years and the number density of ambient gas is $\sim 0.003 - 0.3$ cm^{-3}. This suggests that the local interstellar medium around the SNR is low.

Subject headings: galaxies: individual (M31) — supernova remnants — X-rays: ISM

1. INTRODUCTION

X-ray emission from supernova remnants (SNRs) in our Galaxy has been extensively studied in the past twenty years. Pre-*Chandra* observations allowed many SNRs to be resolved, revealing several different morphologies. The detailed study of SNR morphology has revealed the interaction of ejected materials with the interstellar medium (ISM) in detail, and also has provided insights into the evolution of the SNR progenitor stars. *Chandra* observations of Galactic SNRs provide exquisite detail, allowing the chemical stratification of the progenitor to be revealed (e.g., Canizares et al. 2001) and identifying the central neutron star and its associated synchrotron nebula (e.g., Slane et al. 2000). Even with these new insights, studies of Galactic SNRs can be limited by the lack of reliable distance estimates and generally high interstellar absorption. These limitations are overcome by studies of SNRs in nearby extragalactic systems, the closest of which (the Large and Small Magellanic Clouds) are near enough to still allow *Chandra* to reveal the structure in detail (see e.g., Hughes 2001).

Because M31 is the closest ($\sim$ 800 kpc) galaxy which shares similar morphology and size with the Milky Way, it is the best candidate for a comparative study of SNR. Optical surveys for SNR in M31 typically identify candidates based on [S II] and H_α imaging observations, e.g. d'Odorico, Dopita, & Benvenuti (1980), Blair, Kirshner, & Chevalier (1981, 1982), Braun & Walterbos (1993) and Magnier et al. (1995). About 200 SNR candidates have been identified by these surveys, 27 of which have been confirmed via spectroscopic observations (see Blair et al. 1981, 1982). In a recent extensive *ROSAT* PSPC survey (Supper et al. 2001) of M31, 16 SNRs were identified within a total area of ~ 10.7 deg^2 by cross-correlating with the these optical catalogs. Their X-ray luminosities (0.1–2.4 keV) range from $\sim 10^{36}$ to $\sim 10^{37}$ erg s^{-1}.

More recently, Kong et al. (2002) detected two SNRs (CXOM31 J004327.7+411829 and CXOM31 J004253.5+412553) in the central $\sim 17' \times 17'$ region of M31 with *Chandra*, both of which were previously identified by *ROSAT*. It is worth noting that CXOM31 J004327.7+411829 was also identified as a SNR in the *Einstein* data (Blair et al. 1981). In a recent *Chandra* observation of M31 core region, we found that one of the SNRs is extended. In this Letter, we report on observations of the first SNR in M31 to be resolved at X-ray wavelengths, CXOM31 J004327.7+411829.

2. OBSERVATIONS AND DATA REDUCTION

CXOM31 J004327.7+411829 was observed several times with *Chandra* Advanced CCD Imaging Spectrometer (ACIS-I) under a M31 monitoring program during 1999–2001 (see Kong et al. 2002). CXOM31 J004327.7+411829 is about $8'$ from the aim point of these observations, and therefore the instrumental point spread function (PSF) is substantially poorer than if it was on-axis. In a recent 5ks ACIS-I observation of a transient in M31 taken on 2001 August 31 (Kong et al. 2001), CXOM31 J004327.7+411829 is $< 4'$ from the aim-point, where the PSF is sufficiently small to allow us to resolve this object. Additional observations were obtained with the ACIS-S on 2001 October 5 with total integration time of 37.7ks; although CXOM31 J004327.7+411829 is in the ACIS-S4 front-illuminated (FI) chip and is almost $8'$ from the aim-point, this long observation provides nearly 300 counts and allows the best study of the source spectrum. In this Letter, we concentrate on the analysis of these two latterly mentioned observations; we also make use of other short ($\sim$ 5ks) ACIS observations (see e.g., Di Stefano et al. 2002; Kong et al. 2002) to construct the long-term lightcurve.

All ACIS data were telemetered in Faint mode, and were collected with frame transfer time of 3.2 s. In order to reduce the instrumental background, we screened the data to allow only photon energies in the range of 0.3–7 keV, and *ASCA* grades of 0, 2, 3, 4, and 6. In addition, ~ 300 s of data was excluded from the 2001 October 5 observations due to increased background (likely due to increased particle flux from the solar wind). Data were reduced and analyzed with the *Chandra* X-ray Center CIAO v2.2 package [1] and spectral analysis was performed by making use of XSPEC v11.2 [2]. Unless otherwise specified, all quoted errors are at the 1σ level.

3. ANALYSES AND RESULTS

[1] http://asc.harvard.edu/ciao/

[2] http://heasarc.gsfc.nasa.gov/docs/xanadu/xspec/index.html

3.1. *X-ray Image*

CXOM31 J004327.7+411829 was clearly detected in both observations, but we determined the source position and morphology from the shorter 5ks image because the source was significantly closer to the aimpoint in this dataset. We examined the aspect of this observation with the thread provided by the CXC [3]; and find an offset of 1.34″ and –1.43″ in R.A. and Dec., respectively. After correcting for this aspect offset, the coordinates of the center of CXOM31 J004327.7+411829 are found to be R.A.=$00^h\,43^m\,27.8^s$, DEC.=+41°18′ 29″ (J2000) with a positional error of about 0.5″. The optical counterpart of CXOM31 J004327.7+411829 is source 2-033 in Magnier et al. (1995), source 15 in d'Odorico et al. (1980) and source BA23 in Blair et al. (1981). This object was identified as an irregular, faint and high [S II]/H_α (~ 1) SNR. The optical extension is about $10'' - 18''$, with a slight elongation along the DEC. direction. This source was previously detected (but not resolved) with the *ROSAT* PSPC and identified as an SNR (Supper et al. 1997,2001, source RX J0043.4+4118). It was out of the field-of-view of the *ROSAT* HRI search for SNR in M31 which might have resolved it (Magnier et al. 1997). Figure 1 shows the "true color" X-ray image of CXOM31 J004327.7+411829. The color scheme is defined as 0.5–0.8 keV = red, 0.8-1.2 keV = green, and 1.2–4 keV = blue. The choice of such energy ranges is to highlight the O and Ne/Fe emissions (see § 3.2) from the SNR. CXOM31 J004327.7+411829 is clearly extended in X-rays as a distinct ring-shaped object with a diameter of $\sim 11''$ (42 pc at 780 kpc). The uncertainty of physical dimension of the SNR is dominated by the distance to M31; for instance, Supper et al. (1997,2001) used 690 kpc, corresponding to ~ 37 pc. Our quoted distance (780 kpc; Stanek & Garnavich 1998) is the upper end of all distance estimates.

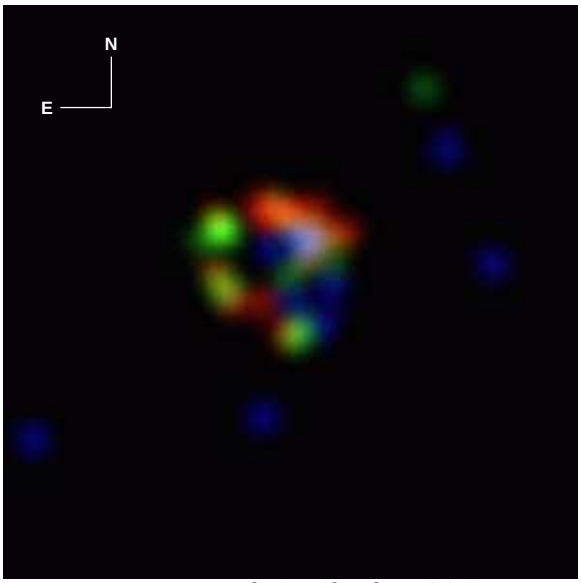

Figure 1: "True color" *Chandra* ACIS-I image of CXOM31 J004327.7+411829. This image was constructed from the soft (red: 0.5–0.8 keV), medium (green: 0.8–1.2 keV) and hard (blue: 1.2–4 keV) energy bands. The pixel size is 0.496″ and the image has been slightly smoothed with a 0.8″σ Gaussian function. The diameter of the SNR is about 11″.

[3]http://asc.harvard.edu/mta/ASPECT/fix_offset/fix_offset.cgi

[4]see http://asc.harvard.edu/cal/Links/Acis/acis/Cal_prods/qeDeg/

[5]http://www.astro.psu.edu/users/chartas/xcontdir/xcont.html

3.2. *Spectral Analysis*

The long 37.7 ks ACIS observation was used for spectral analysis. We extracted data from a circle of 12 pixels ($\sim 6''$) radius centered on CXOM31 J004327.7+411829 and background from an annulus with inner and outer radii of 30 and 60 pixels, respectively. We found 266 net source counts. In order to allow χ^2 statistics to be used, the spectrum was grouped into at least 15 counts per spectral bin. Response files were selected according to the CCD temperature with standard CIAO routines. We fit the data with several single-component spectral models including power-law, thermal bremsstrahlung, blackbody, Raymond-Smith (RS) and non-equilibrium ionization (NEI) models with interstellar absorption. The RS model is a simple collisional equilibrium ionization model, while NEI model is appropriate for modeling SNRs whose age is smaller than the time required to reach ionization equilibrium. NEI model consists of electron temperature (kT_e) and ionization timescale ($\tau = n_e t$), where n_e and t are the mean electron density and the elapsed time after the plasma was shock heated to a constant temperature kT_e. Both models are often applied to study X-ray emission from extragalactic SNRs (see e.g., Wang 1999; Schlegel, Blair, & Fesen 2000; Hughes, Hayashi, & Katsuji 1998). We were also concerned that the quantum efficiency degradation of ACIS will affect our spectral fit[4]. The degradation is shown to be a function of time and is most severe at low energies. We therefore applied corrections using the ACISABS absorption model in XSPEC [5]. This model allows us to correct the response by inputing the number of days between *Chandra*'s launch and the observation (805 days for our observation). In general, the degradation mainly affects the best fit N_H, which is over-estimated without the correction. All results reported here are corrected for the degradation.

Except for the RS and NEI models, other spectral models give unacceptable fits to the data ($\chi^2/\nu > 2$). For the RS and NEI models, we first fixed the abundances at solar value (Andens & Grevesse 1989). We also did fits with the abundances of O, N, and Fe as free parameters and the remaining elements fixed to the solar value. Finally, we fixed the abundances based on optical spectroscopy of CXOM31 J004327.7+411829 with to be 2.3×10^{-4} (O), 8.4×10^{-5} (N) and 0.72×10^{-5} (S) relative to hydrogen, respectively (Blair et al. 1982); these correspond to 0.27, 0.75, and 0.44 solar abundance. Table 1 lists the best-fitting parameters for the RS and NEI models.

All models except the RS model fixed at the optically determined abundances provide acceptable fits. The NEI models clearly have relatively large errors, especially the electron temperature, kT_e. The best-fit N_H is slightly lower (within 1σ) than the Galactic value along the direction (7×10^{20} cm^{-2}; Dickey & Lockman 1990), and the lower limit is not well constrained. Moreover, the abundance of O, Ne, and Fe is not constrained if they are left as free parameters in the NEI model. The best fit temperatures of the RS models with solar abundances and free O, Ne and Fe abundances are similar. The N_H for the models with solar abundances is an order of magnitude greater than the optically determined value (see below). The X-ray spectrum with an absorbed RS model is shown in Figure 2. It is evident that the spectrum is dominated by a broad emission line of O VIII at 0.654 keV and a blend of Fe L shell lines and Ne K shell lines around 0.9 keV.

TABLE 1
BEST-FITTING SPECTRAL PARAMETERS

Model	N_H ($\times 10^{21}$ cm^{-2})	kT_{RS}/kT_e (keV)	$\log n_e t$	Abundance[a] N	O	Ne	S	Fe	L_X [b]	χ^2_ν/d.o.f
RS	$6.78^{+0.49}_{-0.56}$	$0.14^{+0.03}_{-0.01}$		1	1	1	1	1	20.7	1.06/13
RS	$4.60^{+0.96}_{-2.11}$	$0.18^{+0.07}_{-0.02}$		1	$0.49^{+0.39}_{-0.19}$	$0.78^{+0.54}_{-0.26}$	1	$0.14^{+0.12}_{-0.09}$	4.5	0.89/10
RS	$5.88^{+0.50}_{-0.53}$	$0.14^{+0.03}_{-0.01}$		0.75[c]	0.27[c]	1	0.44[c]	1	13.4	1.64/13
NEI	$0.21^{+0.65}_{-0.21}$	$2.1^{+5.6}_{-0.7}$	$10.3^{+0.19}_{-0.16}$	1	1	1	1	1	0.32	0.83/12
NEI	$0.25^{+0.62}_{-0.25}$	$2.1^{+5.6}_{-0.45}$	$10.3^{+0.19}_{-0.16}$	0.75[c]	0.27[c]	1	0.44[c]	1	0.32	0.83/12

NOTE.—All quoted uncertainties are 1σ. ACISABS model is applied to correct the degradation of ACIS (see text).

[a]Relative to the solar abundance.

[b]0.3–7 keV luminosity ($\times 10^{37}$ erg s^{-1}), assuming a distance of 780 kpc; Stanek & Garnavich 1998.

[c]Fixed at optical value (Blair et al. 1982).

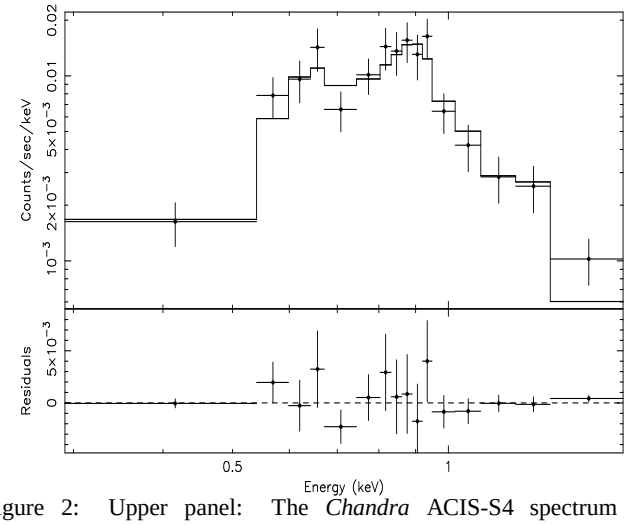

Figure 2: Upper panel: The *Chandra* ACIS-S4 spectrum of CXOM31 J004327.7+411829 with an absorbed RS model ($N_H = 4.6 \times 10^{21}$ cm^{-2}, $kT_{RS} = 0.18$ keV). Lower panel: Residuals after subtracting the fit from the data in units of counts s^{-1} keV^{-1}.

The hydrogen absorption column density for the remnant from optical observations was estimated to be $N_H = 7 \times 10^{20}$ cm^{-2} ($A_V = 0.4$; Blair et al. 1981, 1982). The best fit value for N_H from the RS (NEI) model is higher (slightly lower) than the optically determined value. We also fixed N_H at 7×10^{20} cm^{-2} and the fit is still acceptable, but gives a slightly higher thermal temperature for both models.

3.3. *Lightcurve*

The long-term lightcurve is shown in Figure 3, which is constructed from a series of ACIS pointings (see e.g., Di Stefano et al. 2002; Kong et al. 2001). The background subtracted count rate was corrected for exposure, background variation and instrumental PSF. The mean count rate is 0.007 count s^{-1} and it is evident that the source does not vary significantly as expected for a SNR.

We also tested for variability over shorter time scales during the 37.7 ks observation. We binned the data into 500 s, 1000 s, 5000 s and 10000 s resolution and used Kolmogorov-Smirnov test to search for variability, finding nothing significant.

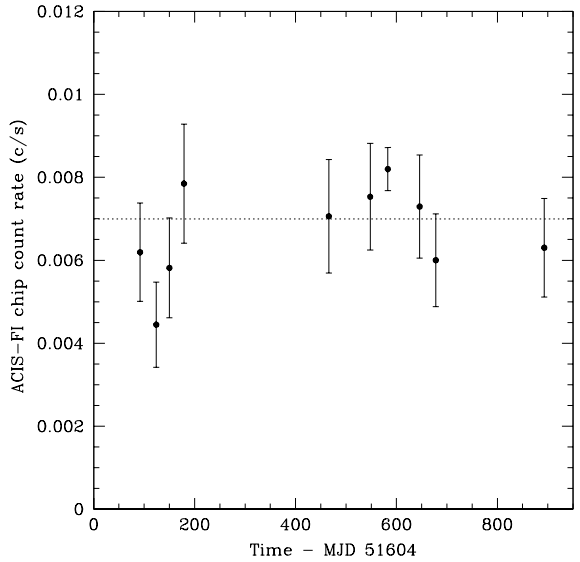

Figure 3: Lightcurve of the *Chandra* count rate in the 0.3–7 keV range of CXOM31 J004327.7+411829 since 2000 March. The horizontal line is the average count rate of the SNR.

4. DISCUSSION

CXOM31 J004327.7+411829 is clearly resolved with *Chandra* into a ring-shaped object. This is the first extragalactic SNR resolved at X-ray wavelengths (other than those in the Large and Small Magellanic Clouds). The diameter of CXOM31 J004327.7+411829 as measured by *Chandra* is about 11″, corresponding to 42 pc; this is comparable to the optically determined value (d'Odorico et al. 1980; Blair et al. 1981). The X-ray image shows evidence of a spatial dependence of chem-

ical composition, with O concentrating in the north-western part, and Ne/Fe distributing along the eastern and south-eastern arc. It is unclear if the X-ray image shows the "blow out" seen in the south-eastern section of the optical image (d'Odorico et al. 1980; Maginer et al. 1995). There is no significant variability on both long (months to years) and short (hours) time scales. The X-ray emission from CXOM31 J004327.7+411829 can be acceptably fit with a RS model. For abundances fixed at solar values, the estimated luminosity is near the Eddington luminosity for a $1.4M_{\odot}$ neutron star, which makes this SNR one of the most luminous ($> 10^{38}$ erg s^{-1}) objects in M31 (see Kong et al. 2002). Beacaue it is not realistic to assume solar abundances for all elements, we here consider the RS model with varing chemical abundances. Fits to RS model with variable abundances find a slightly lower X-ray luminosity of $\sim 5 \times 10^{37}$ erg s^{-1} (0.3–7 keV; $N_H = 4.6 \times 10^{21}$ cm^{-2} and temperature $kT_{RS} = 0.18$ keV), which is at the high end of luminosity distribution of SNR in M31 (Supper et al. 1997; Magnier et al. 1997). Assuming CXOM31 J004327.7+411829 is in the adiabatic expansion phase, we can estimate its physical parameters through the Sedov solution:

$$R = 5\,\mathrm{pc} \times (E_{51} t_3^2 / n_0)^{1/5}, \quad (1)$$

where $R, E_{51}, t_3,$ and n_0 are the radius (in pc), initial explosion energy (in units of 10^{51} erg), age (in units of 1000 yr), and number density of ambient gas (in units of cm^{-3}) of the SNR, respectively. The shock temperature can be written as

$$T_s = (0.18\ \mathrm{keV})(R/t_3)^2, \quad (2)$$

Adopting a radius of 21 pc, $T_s = 0.18$ keV, and $E_{51} = 0.465$ (Blair et al. 1981); from equations (1) and (2), We obtain $t = 21000$ years and $n_0 = 0.16$ cm^{-3}. Considering the SNR's size and uncertainty of spectral fit, t ranges between 15700 years and 22300 years while n_0 varies between 0.11 cm^{-3} and 0.26 cm^{-3}. We therefore can classify CXOM31 J004327.7+411829 as a middle-aged SNR (cf e.g., Hughes et al. 1998) based on the age derived from the X-ray spectrum. Because SNR sometimes contain a pulsar and/or a pulsar nebula we also did some fits including a power-law component with photon index fixed at 2 along with our RS model. These fits limit the power-law component to less than about 25% of the flux. From the derived density, the swept-up mass is estimated to be $(4/3)M_H n_0 \pi R^3 \sim 153 M_{\odot}$, where M_H is mass of a hydrogen atom. Taking into account of the uncertainty of the SNR's size and temperature, the swept-up mass ranges from $105M_{\odot}$ to $172M_{\odot}$. Thus for an ejected mass of a few solar masses, the ratio of swept-up to ejected mass is $\sim 20-30$, indicating that the SNR is in the Sedov phase.

The X-ray emission from CXOM31 J004327.7+411829 can also be fit with an absorbed NEI model although the uncertainties of N_H and kT_e are large. Using this model, the X-ray luminosity (0.3–7 keV) of the SNR is estimated to be $\sim 3 \times 10^{36}$ erg s^{-1}, which is typical of SNR in M31. Using Eqns (1) and (2), we obtain $t = 3210-7530$ years and $n_0 = 0.003-0.02$ cm^{-3}. The ratio of swept-up to ejected mass is ~ 5, indicating that the SNR might be in the early Sedov phase. Comparing to RS model, these values are smaller. In particular, the number density of ambient gas is very low. The relatively high kT_e (= 2.1 keV) is not unusual; for example, N132D in the Large Magellanic Cloud requires a two-component NEI model for which the temperatures are 0.8 and 2.7 keV (Favata et al. 1997). The usual explanation for the hot component is that it comes from the shock-heated swept-up circumstellar medium, or it is due to the inhomogeneity of the ISM.

The number density of ambient gas is relatively low ($n_0 = 0.003-0.26$ cm^{-3}). For example, from a well-studied sample of SNRs in the Large Magellanic Cloud (e.g. Hughes et al. 1998), n_0 ranges between 0.3 to 4 cm^{-3}. Previous *ROSAT* observations of M31 indicate that the number of X-ray emitting SNRs is surprisingly small (Supper et al. 1997; Magnier et al. 1997); only 16 out of 200 optically identified SNRs were detected in X-rays. Magnier et al. (1997) suggested that this lack of X-ray emission could be due to lower than expected local ISM densities, i.e., non-detected SNRs may be in regions with densities less than 0.1 cm^{-3}, while those SNR detected in X-rays may be in higher density regions. The low n_0 we find for CXOM31 J004327.7+411829 provides support for this suggestion. In addition, in the optical image of Magnier et al. (1995), the SNR appears to be away from high density regions of the galaxy, suggesting that it may be in a relatively low density region.

Magnier et al. (1997) note that a multi-component ISM model (McKee & Ostriker 1977) is required for M31. In this case the densities we derive herein may be upper limits to the dominant low-density component of the ISM in the vicinity of the SNR. A future longer observation with the SNR on-axis is required to investigate multi-component model and detailed morphology.

We thank Bryan Gaensler and Patrick Slane for discussions, and an anonymous referee for useful comments. AKHK was supported by NASA LTSA Grants NAG5-10889 and NAG5-10705. MRG acknowledges the support of NASA LTSA Grant NAG5-10889 and NASA Contract NAS8-39073 to the CXC. The HRC GTO program is supported by NASA Contract NAS-38248. We acknowledge the hospitality of the Aspen Center for Physics, which allowed parts of this paper to be written.

REFERENCES

Andens, E., & Grevesse, N. 1989, Geochimica et Cosmochinica Acta, 53, 197
Blair, W.P., Kirshner, R.P., & Chevalier, R.A. 1981, ApJ, 247, 879
Blair, W.P., Kirshner, R.P., & Chevalier, R.A. 1982, ApJ, 254, 50
Canizares, C.R., Flanagan, K.A., Davis, D.S., Dewey, D., & Houck, J.C., Schattenburg, M. L. 2001, in Young Supernova Remnants. Eleventh Astrophysics Conference held October 16-18, 2000, in College Park, MD. Edited by Stephen S. Holt and Una Hwang. AIP Conference Proceedings Volume 565, ISBN 0-7354-0001-6. Published by the American Institute of Physics, Melville, New York, 2001, p.213
Dickey, J.M., & Lockman, F.J. 1990, ARA&A, 28, 215
Di Stefano, R., Kong, A.K.H., Garcia, M.R., Barmby, P., Greiner, J., Murray, S.S., & Primini, F.A. 2002, ApJ, 570, 618
d'Odorico, S., Dopita, M.A., & Benvenuti, P. 1980, A&AS, 40, 67
Favata, F., Vink, J., Parmar, A.N., Kaastra, J.S., & Mineo, T. 1997, A&A, 324, L45
Hughes, J. 2001, in Young Supernova Remnants. Eleventh Astrophysics Conference held October 16-18, 2000, in College Park, MD. Edited by Stephen S. Holt and Una Hwang. AIP Conference Proceedings Volume 565, ISBN 0-7354-0001-6. Published by the American Institute of Physics, Melville, New York, 2001, p.419 (astro-ph/0102377)
Hughes, J.P., Hayashi, I., & Koyama, K. 1998, ApJ, 505, 732
Kong, A.K.H., Garcia, M.R., Primini, F.A., Murray, S.S., Di Stefano, R., & McClintock, J.E. 2002, ApJ, 577, 738
Kong, A.K.H., Garcia, M.R., Murray, S.S., Primini, F.A., McClintock, J.E., & Di Stefano, R. 2001, ATel 76
Magnier, E.A., Prins, S., van Paradijs, J., Lewin, W.H.G., Supper, R., Hasinger, G., Pietsch, W., & Trumper, J. 1995, A&AS, 114, 215

Magnier, E.A., Primini, F.A., Prins, S., van Paradijs, J., & Lewin, W.H.G. 1997, ApJ, 490, 649
McKee, C.F., & Ostriker, J.P. 1977, ApJ, 218, 148
Schlegel, E.M., Blair, W.P., & Fesen, R.A. 2000, AJ, 120, 791
Slane, P. Chen, Y, Schulz, N.S., Seward, F.D., Hughes, J.P., & Gaensler, B.M. 2000, ApJ, 533, L29
Stanek, K.Z., & Garnavich, P.M. 1998, ApJ, 503, L131
Supper, R., Hasinger, G., Pietsch, W., Trumper, J., Jain, A., Magnier, E.A., Lewin, W.H.G., & van Paradijs, J 1997, A&A, 317, 328
Supper, R., Hasinger, G., Lewin, W.H.G., Magnier, E.A., van Paradijs, J., Pietsch, W., Read, A.M., & Trumper, J. 2001. A&A, 373, 63
Wang Q.D. 1999, ApJ, 517, L27